Effects of tofacitinib in early arthritis-induced bone loss in an adjuvant-induced arthritis rat model

Vidal B.[1], Cascão R.[1], Finnilä MA.[2,3], IP. Lopes[1], da Glória VG.[1], Saarakkala S.[2,4], Zioupos P.[5], Canhão H.[6], Fonseca JE.[1,7]

1 Instituto de Medicina Molecular, Faculdade de Medicina, Universidade de Lisboa, Lisbon, Portugal; 2 Research Unit of Medical Imaging, Physics and Technology, Faculty of Medicine, University of Oulu, Oulu, Finland; 3 Department of Applied Physics, University of Eastern Finland, Kuopio, Finland; 4 Medical Research Center, University of Oulu, Oulu, Finland; 5 Biomechanics Labs, Cranfield Forensic Institute, Cranfield University, DA of the UK; ; 6 EpiDoC Unit, CEDOC, NOVA Medical School, NOVA University, Lisbon, Portugal; 7 Rheumatology Department, Centro Hospitalar de Lisboa Norte, EPE, Hospital de Santa Maria, Lisbon Academic Medical Centre, Lisbon, Portugal

ABSTRACT

Rheumatoid arthritis (RA) causes immune mediated local and systemic bone damage. **Objectives** - The main goal of this work was to analyze, how treatment intervention with tofacitinib prevents the early disturbances on bone structure and mechanics in adjuvant induced arthritis rat model. This is the first study to access the impact of tofacitinib on the systemic bone effects of inflammation. **Methods** - Fifty Wistar adjuvant-induced arthritis (AIA) rats were randomly housed in experimental groups, as follows: non-arthritic healthy group (N=20), arthritic non-treated (N=20) and 10 animals under tofacitinib treatment. Rats were monitored during 22 days after disease induction for the inflammatory score, ankle perimeter and body weight. Healthy non-arthritic rats were used as controls for comparison. After 22 days of disease progression rats were sacrificed and bone samples were collected for histology, micro computed tomography (micro-CT), 3-point bending and nanoindentation analysis. Blood samples were also collected for bone turnover markers and systemic cytokine quantification. **Results** - At tissue level, measured by nanoindentation, tofacitinib increased bone cortical and trabecular hardness. However, micro-CT and 3-point bending tests revealed that tofacitinib did not revert the effects of arthritis on cortical and trabecular bone structure and on mechanical properties. **Conclusion** - Possible reasons for these observations might be related with the mechanism of action of tofacitinib, which leads to direct interactions with bone metabolism, and/or with kinetics of its bone effects that might need longer exposure.

KEYWORDS: Rheumatoid arthritis, bone, inflammation, DMARD, animal models.

Corresponding author: Bruno Vidal, Instituto de Medicina Molecular, Faculdade de Medicina da Universidade de Lisboa. Av. Professor Egas Moniz 1649-028 Lisboa, Portugal, T +(351) 217 999 411; Email: vidal.bmc@gmail.com

INTRODUCTION

Rheumatoid arthritis (RA) is a chronic immune-mediated inflammatory disease, which affects around 1% of the world-population.[1] It causes joint and systemic inflammation that is reflected in local and systemic bone damage.[2] In fact, as RA progresses there is marked bone destruction, with radiological evidence of bone erosion within 2 years of disease onset.[3] In addition, osteoporosis is a common finding in patients with RA.[4] This is responsible for increased rates of vertebral and hip fractures in these patients.[5, 6] RA is associated with an increased expression of the receptor activator of nuclear factor kappa–B ligand (RANKL) and low levels of its antagonist, osteoprotegerin (OPG).[7] RANKL is a crucial activator of osteoclastogenesis.[8] In addition, RA serum and synovial fluid present an inflammatory cytokine profile, including interleukin (IL) 1β, IL6, IL17 and tumour necrosis factor (TNF), which further favors osteoclast differentiation and activation since the early phase of the disease.[9-11] Evidence suggests that bone remodeling imbalance in RA contribute not only to local bone erosions but also to the development of systemic osteoporosis.[12]

We have previously found in the adjuvant-induced arthritis (AIA) rat model that 22 days of inflammatory disease progression directly led to the degradation of bone biomechanical

1

properties, namely stiffness, ductility and bone strength, which was paralleled by a high collagen bone turnover.[13]

Tofacitinib is a selective inhibitor of janus kinase 1 (JAK1) and janus kinase 3 (JAK 3), thus interfering with the dimerization of signal transducer and activator of transcription (STAT) molecules, blocking the activation of gene transcription that is dependent on the JAK-STAT signaling pathway.[14-16] Tofacitinib is in its final approval steps by EMA for the indication of RA treatment.[17] The main goal of this work was to analyze, if treatment intervention with tofacitinib in the AIA rat model prevents the early disturbances on bone structure and strength induced by inflammation.

METHODS

Animal experimental design

Fifty 8 week-old female Wistar AIA Han rats weighing approximately 200-220gr were housed in European type II standard filter top cages (Tecniplast, Buguggiate, Italy) and transferred into the SPF animal facility at the Instituto de Medicina Molecular, Faculdade de Medicina, Universidade de Lisboa, under a 14h light/10h dark light cycle, acclimatized to T= 20-22ºC and RH= 50-60%. They were given access to autoclaved rodent breeder chow (Special Diet Service, RM3) and triple filtered water. AIA rats were purchased from Charles River laboratories international (Barcelona, Spain) and they were delivered at Instituto de Medicina Molecular after three days of disease induction.

Sample size was calculated using the Power Analysis statistical test from the G * Power 3.1 software (http://www.gpower.hhu.de). The test was based on our own previous data, [13] comparing the medians of the experimental groups using the Mann-Whitney test, with alpha (probability of error) = 0.05, power = 95%, effect size = 1.751632 and actual power = 0.95072 (calculated from previous experimental data; http://www.polyu.edu.hk/mm/effectsizefaqs/calculator/calculator.html).

Upon arrival, animals were randomly housed in groups, individually identified and cages were labelled according to the experimental groups, as follows: non-arthritic healthy group (N=20), arthritic treated with tofacitinib (10mg/kg body weight, by oral gavage, twice a week) (N=10) and arthritic non-treated (received an equal volume of vehicle, 0.5% methylcellulose in water) (N=20). Tofacitinib administration was started 4 days after disease induction, when animals already presented clinical signs of arthritis. The inflammatory score, ankle perimeter and body weight were measured during the period of treatment. Inflammatory signs were evaluated by counting the score of each joint in a scale of 0 – 3 (0 – absence; 1 – erythema; 2 – erythema and swelling; 3 – deformities and functional impairment). The total score of each animal was defined as the sum of the partial scores of each affected joint. Rats were sacrificed 22 days post disease induction, as maximum disease activity and severity occurs at day 19, plateaus up to day 22 post disease induction and after that inflammatory signs disappear.[18] Blood, paws and bone samples were collected.

All experiments were approved by the Animal User and Ethical Committees at the Instituto de Medicina Molecular (Lisbon University), according to the Portuguese law and the European recommendations.

Histological evaluation of hind paws

Left hind paw samples collected at the time of sacrifice were fixed immediately in 10% neutral buffered formalin solution and then decalcified in 10% formic acid. Samples were then dehydrated and embedded in paraffin, serially sectioned at a thickness of 5 µm. Sections were stained with hematoxylin and eosin for histopathological evaluation of structural changes and cellular infiltration. This evaluation was performed in a blind fashion using 5 semi-quantitative scores:

• Sublining layer infiltration score (0—none to diffuse infiltration; 1—lymphoid cell aggregate; 2—lymphoid follicles; 3—lymphoid follicles with germinal center formation);

• Lining layer cell number score (0—fewer than three layers; 1—three to four layers; 2—five to six layers; 3—more than six layers);

• Bone erosion score (0—no erosions; 1—minimal; 2—mild; 3—moderate; 4—severe);

• Cartilage surface (0 –normal; 1 – irregular; 2 – clefts; 3 – clefts to bone);

• Global severity score (0—no signs of inflammation; 1—mild; 2—moderate; 3—severe).[19]

Images were acquired using a Leica DM2500 (Leica Microsystems, Wetzlar, Germany) microscope equipped with a colour camera.

Immunohistochemical staining of osteocalcin positive cells in hind paws

Osteoblasts immunolocalization was performed by staining with osteocalcin primary antibody (Abcam, Cambridge, UK) followed by EnVision+ (Dako, Glostrup, Denmark). Color was developed in solution containing diaminobenzadine-tetrahydrochloride (DAB, Sigma, Missouri, USA), 0.5% H_2O_2 in phosphate-buffered saline buffer (pH 7.6). Slides were counterstained with hematoxylin and mounted. Immunohistochemical evaluation of rat joints were performed in a blinded fashion using a semi-quantitative score of 0-3 (0 — 0-25% staining; 1 — 26-50% staining; 2 — 51-75% staining; 3 — more than 75% staining)[20].

Images were acquired using a Leica DM2500 (Leica Microsystems, Wetzlar, Germany) microscope equipped with a colour camera.

STAT1 and suppressor of cytokine signaling 1 (SOCS1) expression in bone

STAT1 and SOCS1 expression were quantified by qPCR in bone tissue (tibia) from untreated (n =14) and tofacitinib treated rats (n=10).

Tibiae were collected after rats sacrifice and stored at -80ºC. On top of dry ice each frozen tibia bone was quickly pulverized with a mortar and pestle, which was previously cooled with liquid nitrogen, to maintain very low temperatures and prevent RNA degradation as described in Carter LE et al., 2012. After pulverization 2ml of Trizol reagent (Invitrogen) was added to the powder and mixture was divided and transferred to two eppendorf tubes, to have at the end 1ml per tube. Trizol protocol was preformed following manufactures instructions.

For qPCR analysis, 1,5 ug of RNA from tibia bone, was DNase I (Roche) treated and reversed transcribed using NZY First-Strand cDNA Synthesis Kit (nzytech) with random hexamer oligos. Real-time quantitative PCR was performed with Power SYBR® Green PCR Master Mix (Applied Biosystems) and gene specific primers for STAT1 (STAT1_ F:5'TTGACAGTATGA TGAGC GCAGT 3'; STAT1_R: 5' TGAAGGAACAGTAGCAGGAAGG 3') and SOCS1 (SOCS1_F: 5' TGGCACGCATCCCTCTTAAC 3'; SOCS1_ R:5'CACTTAATG CTGCGGGCAC3'). PCR was performed in ViiA™ 7 Real-Time PCR System (Applied Biosytems) with an initial step at 50oC for 2 minutes and 95oC for 10 minutes followed by 40 cycles at 95oC for 15 seconds and 60oC for 1 minute. ARBP was used as reference gene (ARBP_F: 5' TCGAAGCAAAGGAAGAG TCGG 3'; ARBP_R: 5' AGGCTGACTTGGTGTGAGGG 3'. CT values were acquired and 2-ΔCT method was used, for analysis.

These genes are affected by JAK kinase inhibition targeted by tofacitinib.

Bone remodeling and inflammatory markers quantification

Serum samples were collected at sacrifice and stored at -80°C. Bone remodeling markers, carboxy-terminal telopeptide of type I collagen (CTX-I) and procollagen type I propeptides (P1NP), were quantified by Serum Rat Laps ELISA assay (Immunodiagnostic Systems Ltd, Boldon, UK).

Proinflammatory cytokines IL-1β, IL-6 (Boster Bio, California, USA), IL-17, OPG, RANKL (Sunred Biological Technology, Shanghai, China) and TNF (RayBiotech, Georgia, USA) were quantified in serum samples using specific rat ELISA kits. Both kits were used following strictly provider's recommendations.

For all biomarkers standard curves were generated by using reference biomarker concentrations supplied by the manufacturers. Samples were analyzed using a plate reader Infinite M200 (Tecan, Mannedorf, Switzerland).

Micro-computed tomography (micro-CT) analysis

Structural properties of the trabecular and cortical tibiae were determined with a high-resolution micro-CT system (SkyScan 1272, Bruker microCT, Kontich, Belgium). Moist bones were wrapped in parafilm and covered with dental wax to prevent drying and movement during the scanning. X-ray tube was set to 50kV and beam was filtered with 0.5mm Aluminum filter. Sample position and camera settings were tuned to provide 3.0µm isotropic pixel size and projection images were collected every 0.2°. Tissue mineral density values were calibrated against hydroxyapatite phantoms with densities of 250mg/cm^3 and 750mg/cm^3. Reconstructions were done with NRecon (v 1.6.9.8; Bruker microCT, Kontich, Belgium) where appropriate corrections to reduce beam hardening and ring artifacts were applied. Bone was segmented in slices of 3µm thickness. After 200 slices from growth plate, we selected and analyzed1400 slices of trabecular bone. For cortical bone, 300 slices (1800 slices from growth plate) were analyzed.

Analyses were performed in agreement with guidelines for assessment of bone microstructure in rodents using micro-computed tomography.[21] Trabecular bone morphology was analyzed by applying global threshold and despeckle to provide binary image for 3D analyzes. For cortical bone ROI was refined with ROI-shrink wrap operation. This was followed by segmentation of blood vessels using adaptive thresholding. Blood vessels and porosity were analyzed using 3D morphological analyses.

Bone mechanical tests

Femurs were subjected to a 3-point bending test using a universal materials testing machine (Instron 3366, Instron Corp., Massachusetts, USA). Femurs were placed horizontally anterior side upwards on a support with span length of 5mm. The load was applied with a constant speed of 0.005mm/s until failure occurred. Stiffness was analyzed by fitting first-degree polynomial function to the linear part of recorded load deformation data. A displacement of 0.15µm between fitted slope and measured curve was used as criteria for yield point, whereas the breaking point was defined as set where force reached maximal value. Force, deformation and absorbed energy were defined at both yield and at the breaking point.

Nanoindentation

Nanoindentation was performed using a CSM-Nano Hardness Tester System (CSM Instruments SA; Switzerland; Indentation v.3.83) equipped with a Berkovich based pyramid diamond tip. After micro-CT, 0.5mm of top tibia was cut and proximal part was embedded to low viscosity epoxy resin (EpoThin, Buehler, Knorring Oy Ab, Helsinki, Finland). Slow speed diamond saw was used to remove 10% of bone length. The sample surface was polished using silicon carbide sandpaper with a decreasing grid size (800, 1200, 2400 and 4800) and finished with cloth with containing 0.05 µm γ-alumina particles. Indentation protocol was adopted from previous work[22] and on average 8 indentations were done on both cortical and trabecular bone with a quasi-static (CSM called 'advanced') loading protocol. All indentations were performed under an optical microscope to achieve the precise location of indentations at the center of the targeted area in the tissue.[23]

In the 'advanced' protocol, a trapezoidal loading waveform was applied with a loading/unloading rate of 20mN/min and with an intermediate load-hold-phase lasting 30s hold at a maximum load 10 mN. The hardness (H_{IT}), indentation modulus (E_{IT}), indentation creep (C_{IT}) and elastic part of indentation work (η_{IT}) were measured by using the Oliver and Pharr (1992) method [24].

Histological images of rat tibiae from diaphyseal cortical region were acquired during the nanoindentation technique, using a CSM instruments (Switzerland) microscope equipped with a color camera.

A histologic score was applied in order to evaluate the lamellar structures of bone tissue. This evaluation was performed in a blind fashion using a semi-quantitative score:

- Lamellar bone structure: (1- predominantly parallel-lamella; 2 - concentric and parallel-lamellae in the same proportion; 3 – predominantly concentric lamella).

The ratio of osteocyte lacuna area / total tissue area was also evaluated at x200 magnification in order to analyse the percentage of total tissue area occupied by osteocyte lacunae. The method of acquisition and analysis used was the same applied for the evaluation of bone volume / tissue volume in histomorphometry technique [13]. All variables were expressed and calculated according to the recommendations of the American Society for Bone and Mineral Research [25], using a morphometric program (Image J 1.46R with plugin Bone J).

Statistical analysis

Statistical differences were determined with Mann–Whitney tests using GraphPad Prism (GraphPad, California, USA). Correlation analysis was performed with the Spearman test. Differences were considered statistically significant for $p < 0.05$.

RESULTS

Tofacitinib effectively reduced inflammation in the AIA rat model of arthritis

Results showed that tofacitinib effectively controlled and abrogated disease development in comparison with untreated arthritic rats (fig.1A). Moreover, untreated arthritic animals sharply increased the ankle perimeter throughout disease progression (fig.1B). Rats under tofacitinib treatment presented an ankle perimeter similar to healthy controls.

Tofacitinib abrogated local joint inflammation and local bone and cartilage damage in AIA rats

To evaluate the effect of tofacitinib treatment in the preservation of joint structure and periarticular bone, paw sections stained with haematoxylin and eosin were performed (illustrative images can be observed in Fig 2A). The histological evaluation using 5 semi-quantitative scores is depicted in Fig 2 (B-F).

Sublining layer infiltration (B) and the number of lining layer cells (C) were lower in the tofacitinib group when compared with the untreated arthritic group at the end of the study ($p < 0.0001$). Tofacitinib was also effective in preventing joint bone erosions (D) and cartilage damage (E) ($p < 0.0001$ and $p = 0.0001$ tofacitinib group vs. arthritic rats, respectively).

Thus, these data reveals that tofacitinib was able to significantly diminish inflammation and local bone damage (Fig. 2F, $p < 0.0001$ tofacitinib group vs. arthritic rats).

In addition, arthritic rats showed increased numbers of osteoblasts (osteocalcin+ cells lining bone surfaces) in the hind paw ($p = 0.0029$ *vs* healthy controls). Tofacitinib administration significantly lowered the number of osteoblasts to levels similar to healthy controls ($p = 0.0035$ *vs* arthritic rats) (Sfig1).

Tofacitinib down-regulates the JAK-STAT pathway in bone tissue

A significant decreased expression of STAT1 (Sfig2 A) and SOCS1 (Sfig2 B) were observed in the bone of AIA rats treated with tofacitinib, in comparison to arthritic untreated rats ($p = 0.0019$ and $p = 0.044$, respectively).

Tofacitinib reduced bone remodeling and inflammatory markers

We have observed that both CTX-I (Fig. 3A) and P1NP (Fig. 3B) were significantly increased in the arthritic group in comparison with the healthy control animals ($p < 0.0001$ and $p = 0.0015$, respectively), revealing an increase of bone turnover in the arthritic group. The tofacitinib group showed decreased values for CTX-I ($p = 0.0002$) and P1NP ($p = 0.0018$) when compared with the arthritic group, suggesting a decreased bone turnover (Fig.3).

RANKL levels were decreased in the serum of tofacitinib-treated rats in comparison with healthy control and untreated arthritic rats ($p = 0.0083$ and $p = 0.0141$, respectively), as observed in Fig 3C. OPG levels were also reduced in tofacitinib group in comparison with healthy control and

untreated arthritic rats (p= 0.0031 and p= 0.0002, respectively)(Fig. 3D). No differences were observed in RANKL/OPG ratio between tofacitinib and arthritic untreated group. The tofacitinib group showed an increased RANKL/OPG ratio when compared to healthy control group (p= 0.0370 Fig. 3E).

We have also quantified the circulating concentration of IL-1β, IL-6 and TNF, but no differences were found when comparing arthritic rats with animals treated with tofacitinib (Fig. 3F, 3G and 3H). However, there was a slight tendency for IL-6 to be diminished in the tofacitinib group when compared with untreated arthritic animals.

Tofacitinib administration significantly reduced the levels of IL-17 detected in peripheral blood, (p<0.0001, tofacitinib group vs. untreated arthritic rats after 22 days of disease induction) (Fig. 3I).

Micro-CT

The effect of tofacitinib on inflammation-induced bone loss was assessed by micro-CT of cortical (Fig 4 A-C) and trabecular (Fig 4 D - I) bone tibia. Arthritic rats showed a reduction in cross-sectional area (A) and thickness (B) and tofacitinib treatment did not restore these cortical changes (p<0.0001 vs healthy controls, respectively). These bone changes affected the ability of bone's torsion as showed by decreased values of polar moment of inertia (C) in arthritic and tofacitinib group (p=0.0059 and p=0.0197 vs healthy controls, respectively). Trabecular bone also presented dramatic deterioration with arthritis as evidenced by a reduced trabecular bone volume fraction (D) (p=0.0007 and p<0.0001 vs healthy controls, respectively), thickness (E) and number (F) (p<0.0001 vs healthy controls) and also by an increased trabecular separation (G) (p<0.0001 in arthritic group and p=0.0002 in tofacitinib group vs healthy controls) and porosity (H) (p<0.0001 vs healthy controls). Furthermore, structure model index (I) showed declined values in arthritic and tofacitinib group (p<0.0001vs healthy controls, respectively) indicating that trabeculae shape was rather rod-like compared to plate-like shape in healthy controls.

Tofacitinib could not rescue trabecular bone integrity and trabecular bone properties in treated rats (Fig.4J).

Three-point bending

Tissue-level mechanical properties of rat femurs were evaluated using 3-point bending mechanical test at the end of the experiment. As shown in Fig. 5, arthritic rats revealed decreased mechanical properties at yield point, namely displacement (p=0.0192 vs healthy controls, Fig 5A), strength (p=0.0229 vs healthy control, Fig 5B) and pre yield energy (elastic energy) (p=0.0161 vs healthy controls, Fig 5C). These results showed that arthritic bones started to accumulate micro fractures with smaller deformations and lower loads, leading to a decreased energy absorption capability at yield point. Tofacitinib treated rats showed a significant decreased displacement (p=0.0039 vs healthy controls, Fig 5D) and elastic properties (p=0.0443 vs healthy controls, Fig 5E) at fracture point, meaning that there was a lower deformation (related to decreased elastic properties) during the plastic phase, before the total fracture of bone. Results also demonstrated that arthritic and tofacitinib rats had decreased maximum load (p= 0.0017 vs healthy controls, Fig 5F). Finally, arthritic rats and the tofacitinib treated group showed a significant decrease in toughness (p=0.0143 and p=0.0048 vs healthy controls, respectively, Fig 5G), demonstrating that arthritic and tofacitinib-treated bone could absorb less energy before fracturing.

Altogether, mechanical data revealed that arthritic and tofacitinib groups had significantly lower mechanical properties as compared to healthy controls, meaning that tofacitinib was unable to abrogate the structural deterioration during the time frame of treatment observed in this animal model.

Tofacitinib increased bone hardness

Nanoindentation was performed in order to assess the quality at tissue matrix level and this technique can be used at the level of a single trabecula or within a confined submicron area of the cortical bone tissue.

Nano-mechanical tests revealed that arthritic rats had decreased hardness in cortical (Fig. 6A) and trabecular bone (Fig. 6B) (p= 0.0010 and p= 0.0080 in arthritic rats vs healthy controls, respectively). In contrast, rats treated with tofacitinib showed restored hardness in cortical bone (Fig. 6A) and increased hardness in trabecular (Fig. 6B) bone (p=0.0003 and p=0.0012 vs untreated arthritic rats, respectively). No differences were observed in the other parameters analysed.

Topographic images gathered during nanoindentation allowed the characterization of bone histologic features from healthy animals, arthritic untreated animals and tofacitinib treated animals after 22 days of disease induction.

Concentric lamellas were identified in secondary osteons (SO) and more frequently observed in arthritic animals (Fig.6 F) than in healthy controls (p= 0.0022) and tofacitinib treated animals (p= 0.0043) (Fig. 6C). On the contrary, healthy animals (Fig. 6 E) and tofacitinib treated animals (Fig. 6 G) presented more parallel-lamellae (PL) structures than concentric lamellas.

In addition, arthritic animals showed an increased area occupied by osteocyte lacunae in the total tissue when compared to healthy animals and tofacitinib treated animals (Fig. 6D) (p=0.0067, p=0.0011, respectively).

DISCUSSION

In this study, we used the AIA rat model to evaluate the efficacy of tofacitinib to treat inflammation as well as inflammation-induced bone damage. Tofacitinib showed significantly reduced arthritis manifestations, synovial tissue inflammation and bone erosions, which was associated with lower serum RANKL and OPG levels. These results are in line with previous observations. [26]

The effects of tofacitinib on pro-inflammatory cytokines production were assessed through serum quantification of IL-1β, IL-6, IL-17 and TNF. Our study depicted decreased levels of IL-17 in AIA rats under tofacitinib treatment in comparison with untreated arthritic animals. In addition, we have observed a tendency towards a decrease in serum IL-6 concentration in tofacitinib treated rats. These observations are expected by tofacitinib inhibition of the JAK and STAT pathways, as verified in bone tissue.[15, 27-29] Tofacitinib did not affect circulating levels of TNF or IL-1β comparing with untreated arthritic rats, but this might be related to the relatively low circulating levels of these cytokines in this animal model.[26]

Biochemical markers of bone turnover were quantified in order to evaluate the impact of tofacitinib on bone metabolism. A reduced bone turnover was shown in tofacitinib treated animals, as depicted by reduced osteoblasts number and decreased CTX-I and P1NP levels.

At tissue level, measured by nanoindentation, tofacitinib increased bone cortical and trabecular hardness. On the contrary, arthritic animals showed decreased values of hardness after 22 days post disease induction. We also observed at day 11 and 22 post arthritis induction concentric lamellas in secondary osteons (SO) microstructures resulting from high bone remodelling, as previously described [13, 30, 31]. Dall'Ara et al. suggested that larger numbers of this younger, less mineralised and less hard structures, could be related to reduced hardness of bone tissue identified by nanoindentation. On the contrary, healthy and tofacitinib treated animals presented more parallel-lamellae (PL) structures than concentric lamellas in SO structures and this PL structures are 10% more harder than the former, representing the mature bone structure (and normal bone remodelling)[31]. In addition, arthritic animals had an increased area occupied by osteocyte lacunae in total tissue. Tofacitinib treated animals, on the contrary, had a normal number of osteocytes lacunae and of the lacunae area per tissue volume. Osteocytes are responsible for the maintenance of the bone homeostasis, regulating the behaviour of osteoblasts and osteoclasts by communicating through gap junctions [32]. Although no previous data is available in the context of arthritis some studies revealed that osteocytes from osteoarthritis patients have an irregular morphology, with limited ability to reply to mechanical stimuli, leading to significant changes in the structure and mineral density [33]. Despite being still unclear, this apparent change of osteocyte morphology in arthritic bone might contribute to the nanomechanical changes observed in this context.

Micro-CT and 3-point bending tests revealed that tofacitinib did not revert the effects of arthritis on cortical and trabecular bone structure and mechanical properties. There are several possible explanations for these observations. Using this same animal model we were able to revert the structural and mechanical damage induced by arthritis using an experimental compound.[19] However, the kinetics of the effects of tofacitinib might be different, needing more exposure time to have an impact on bone quality. The effect at a tissue level might be an early sign of its delayed impact on bone. Of interest, an increase in hardness is associated with a decrease in the relative ratio of elastic-to-plastic behaviour of the tissue and thus it is unclear if it represents ultimately a true improvement in mechanical properties. Another explanation might be related with the mechanism of action. Tofacitinib targets JAK1 and 3, downregulating STAT 1 and 3 of the JAK-STAT signaling pathway,[15, 16, 26] and these intracellular molecules have complex interactions with bone. JAK1 is expressed in bone cells and is involved in bone formation. The depletion of JAK1 promotes bone growth delays, suggesting that JAK1 is critical for skeletal development. On the other hand, STAT1 inhibits Runx2 transcription in osteoblasts, the master transcription factor of osteoblast differentiation. Thus, STAT1 is an inhibitor of differentiation of osteoblasts and the inactivation of STAT1 leads to an osteopetrotic bone phenotype.[34] Consistent with the higher bone mass in STAT1-deficient mice, inactivation of STAT1 can accelerate fracture repair.[35] These data suggest that STAT1 negatively regulates bone formation in vivo.[36] On the contrary, JAK-STAT3 signal transduction pathway promotes osteoblast differentiation [36]. Inactivation of STAT3 in osteoblasts leads to lower bone mass due to inhibition of bone formation. In humans, STAT3 mutations reduce bone mass and increase incidence of minimal trauma fractures. Clinical studies indicate that STAT3 mutations increase osteoclast number and bone resorption, and are associated with recurrent fractures.

It is conceivable that these types of molecular interactions with bone have an overall effect that might not be totally compensated by the benefits on bone obtained by the control of inflammation. Broaden unspecific molecular effects of methotrexate (MTX) potentiate the effect of targeted therapies. This is expected to occur in the combination of MTX with tofacitinib and might contribute, as already explored in clinical trials, to an increment in the inflammatory control, probably fully compensating bone damage. [37] To clarify these open questions it will be relevant to test several doses of tofacitinib and also combination therapy with MTX, in longer duration arthritis models and in healthy animals. In addition, the discrepancy between the effect of tofacitinib on joint erosions and on skeletal bone deserves a fully microstructural study of intra articular bone, compared to skeletal bone.

KEY MESSAGES

- Tofacitinib was able to control and supress inflammatory activity in an AIA rat model of arthritis.

- Tofacitinib wasn't able to revert structural and mechanical bone changes promoted by inflammation.

- JAK-STAT pathway inhibition downregulates several targets which may not be totally beneficial for bone homeostasis.

COMPETING INTERESTS

The authors have declared that no competing interests exist.

REFERENCES

1.   Alamanos Y, Drosos AA. Epidemiology of adult rheumatoid arthritis. Autoimmun Rev. 2005 Mar;4(3):130-6. PubMed PMID: 15823498.

2.   Yelin E, Callahan LF. The economic cost and social and psychological impact of musculoskeletal conditions. National Arthritis Data Work Groups. Arthritis and rheumatism. 1995 Oct;38(10):1351-62. PubMed PMID: 7575685.

3.   Lin YY, Jean YH, Lee HP, Chen WF, Sun YM, Su JH, et al. A soft coral-derived compound, 11-epi-sinulariolide acetate suppresses inflammatory response and bone destruction in adjuvant-induced arthritis. PLoS One. 2013;8(5):e62926. PubMed PMID: 23675440. Pubmed Central PMCID: 3652811.

4.   Haugeberg G, Orstavik RE, Uhlig T, Falch JA, Halse JI, Kvien TK. Bone loss in patients with rheumatoid arthritis: results from a population-based cohort of 366 patients followed up for two years. Arthritis and rheumatism. 2002 Jul;46(7):1720-8. PubMed PMID: 12124854.

5.   Marshall D, Johnell O, Wedel H. Meta-analysis of how well measures of bone mineral density predict occurrence of osteoporotic fractures. BMJ. 1996 May 18;312(7041):1254-9. PubMed PMID: 8634613. Pubmed Central PMCID: 2351094.

6.   Eric-Jan JA K. Bone mass in rheumatoid arthritis. CLINICAL AND EXPERIMENTAL RHEUMATOLOGY. 2000.

7.   Fonseca JE, Cortez-Dias N, Francisco A, Sobral M, Canhao H, Resende C, et al. Inflammatory cell infiltrate and RANKL/OPG expression in rheumatoid synovium: comparison with other inflammatory arthropathies and correlation with outcome. Clin Exp Rheumatol. 2005 Mar-Apr;23(2):185-92. PubMed PMID: 15895888.

8.   Boyle WJ, Simonet WS, Lacey DL. Osteoclast differentiation and activation. Nature. 2003 May 15;423(6937):337-42. PubMed PMID: 12748652.

9.   Moura RA, Cascao R, Perpetuo I, Canhao H, Vieira-Sousa E, Mourao AF, et al. Cytokine pattern in very early rheumatoid arthritis favours B-cell activation and survival. Rheumatology. 2011 Feb;50(2):278-82. PubMed PMID: 21047805.

10.   Cascao R, Moura RA, Perpetuo I, Canhao H, Vieira-Sousa E, Mourao AF, et al. Identification of a cytokine network sustaining neutrophil and Th17 activation in untreated early rheumatoid arthritis. Arthritis research & therapy. 2010;12(5):R196. PubMed PMID: 20961415. Pubmed Central PMCID: 2991033.

11.   Caetano-Lopes J, Canhao H, Fonseca JE. Osteoimmunology--the hidden immune regulation of bone. Autoimmunity reviews. 2009 Jan;8(3):250-5. PubMed PMID: 18722561.

12.   Caetano-Lopes J, Rodrigues A, Lopes A, Vale AC, Pitts-Kiefer MA, Vidal B, et al. Rheumatoid arthritis bone fragility is associated with upregulation of IL17 and DKK1 gene expression. Clin Rev Allergy Immunol. 2014 Aug;47(1):38-45. PubMed PMID: 23546988.

13.   Vidal B, Cascao R, Vale AC, Cavaleiro I, Vaz MF, Brito JA, et al. Arthritis induces early bone high turnover, structural degradation and mechanical weakness. PloS one. 2015;10(1):e0117100. PubMed PMID: 25617902. Pubmed Central PMCID: 4305284.

14.   Tofacitinib. Drugs R D. 2010;10(4):271-84. PubMed PMID: 21171673. Pubmed Central PMCID: 3585773.

15.   Meyer DM, Jesson MI, Li X, Elrick MM, Funckes-Shippy CL, Warner JD, et al. Anti-inflammatory activity and neutrophil reductions mediated by the JAK1/JAK3 inhibitor, CP-690,550, in rat adjuvant-induced arthritis. Journal of inflammation. 2010;7:41. PubMed PMID: 20701804. Pubmed Central PMCID: 2928212.

16.   Maeshima K, Yamaoka K, Kubo S, Nakano K, Iwata S, Saito K, et al. The JAK inhibitor tofacitinib regulates synovitis through inhibition of interferon-gamma and interleukin-17 production by human CD4+ T cells. Arthritis and rheumatism. 2012 Jun;64(6):1790-8. PubMed PMID: 22147632.

17.   AGENCY EM. Eight medicines recommended for approval, including two biosimilars 2017. Available from: http://www.ema.europa.eu/ema/index.jsp?curl=pages/news_ and_events/news/2017/01/news_detail_002682.jsp&mid=WC0b01ac058004d5c1.

18.   Lisa R. Schopf KA, Bruce D. Jaffee. In Vivo Models of Inflammation. Basel/Switzerland: Birkhäuser Basel; 2006.

19.   Cascao R, Vidal B, Raquel H, Neves-Costa A, Figueiredo N, Gupta V, et al. Effective treatment of rat adjuvant-induced arthritis by celastrol. Autoimmun Rev. 2012 Oct;11(12):856-62. PubMed PMID: 22415021. Pubmed Central PMCID: 3582326.

20.   Chen DL, Wang DS, Wu WJ, Zeng ZL, Luo HY, Qiu MZ, et al. Overexpression of paxillin induced by miR-137 suppression promotes tumor progression and metastasis in colorectal cancer. Carcinogenesis. 2013 Apr;34(4):803-11. PubMed PMID: 23275153. Pubmed Central PMCID: 3616669.

21.   Bouxsein ML, Boyd SK, Christiansen BA, Guldberg RE, Jepsen KJ, Muller R. Guidelines for assessment of bone microstructure in rodents using micro-computed tomography. Journal of bone and mineral research : the official journal of the American Society for Bone and Mineral Research. 2010 Jul;25(7):1468-86. PubMed PMID: 20533309.

22.   Herlin M, Finnila MA, Zioupos P, Aula A, Risteli J, Miettinen HM, et al. New insights to the role of aryl hydrocarbon receptor in bone phenotype and in dioxin-induced modulation of bone microarchitecture and material properties. Toxicology and applied pharmacology. 2013 Nov 15;273(1):219-26. PubMed PMID: 24035824.

23.   Zhang R, Gong H, Zhu D, Ma R, Fang J, Fan Y. Multi-level femoral morphology and mechanical properties of rats of different ages. Bone. 2015 Jul;76:76-87. PubMed PMID: 25857690.

24.   W.C. Oliver GMP. An improved technique for determining hardness and elastic modulus using load and displacement sensing indentation experiments1992.

25.   Parfitt AM, Drezner MK, Glorieux FH, Kanis JA, Malluche H, Meunier PJ, et al. Bone histomorphometry: standardization of nomenclature, symbols, and units. Report of the ASBMR Histomorphometry Nomenclature Committee. Journal of bone and mineral research : the official journal of the American Society for Bone and Mineral Research. 1987 Dec;2(6):595-610. PubMed PMID: 3455637.

26.   LaBranche TP, Jesson MI, Radi ZA, Storer CE, Guzova JA, Bonar SL, et al. JAK inhibition with tofacitinib suppresses arthritic joint structural damage through decreased RANKL production. Arthritis and rheumatism. 2012 Nov;64(11):3531-42. PubMed PMID: 22899318.

27.   Milici AJ, Kudlacz EM, Audoly L, Zwillich S, Changelian P. Cartilage preservation by inhibition of Janus kinase 3 in two rodent models of rheumatoid arthritis. Arthritis research & therapy. 2008;10(1):R14. PubMed PMID: 18234077. Pubmed Central PMCID: 2374467.

28.   Tanaka Y, Maeshima K, Yamaoka K. In vitro and in vivo analysis of a JAK inhibitor in rheumatoid arthritis. Annals of the rheumatic diseases. 2012 Apr;71 Suppl 2:i70-4. PubMed PMID: 22460142.

29.   Tanaka Y, Yamaoka K. JAK inhibitor tofacitinib for treating rheumatoid arthritis: from basic to clinical. Modern rheumatology / the Japan Rheumatism Association. 2013 May;23(3):415-24. PubMed PMID: 23212593.

30.   Bailey AJ, Mansell JP, Sims TJ, Banse X. Biochemical and mechanical properties of subchondral bone in osteoarthritis. Biorheology. 2004;41(3-4):349-58. PubMed PMID: 15299267.

31.   Dall'Ara E, Ohman C, Baleani M, Viceconti M. Reduced tissue hardness of trabecular bone is associated with severe osteoarthritis. Journal of biomechanics. 2011 May 17;44(8):1593-8. PubMed PMID: 21496822.

32.   Taylor AF, Saunders MM, Shingle DL, Cimbala JM, Zhou Z, Donahue HJ. Mechanically stimulated osteocytes regulate osteoblastic activity via gap junctions. American journal of physiology Cell physiology. 2007 Jan;292(1):C545-52. PubMed PMID: 16885390.

33.   Jaiprakash A, Prasadam I, Feng JQ, Liu Y, Crawford R, Xiao Y. Phenotypic characterization of osteoarthritic osteocytes from the sclerotic zones: a possible pathological role in subchondral bone sclerosis. International journal of biological sciences. 2012;8(3):406-17. PubMed PMID: 22419886. Pubmed Central PMCID: 3303142.

34.   Kim S, Koga T, Isobe M, Kern BE, Yokochi T, Chin YE, et al. Stat1 functions as a cytoplasmic attenuator of Runx2 in the transcriptional program of osteoblast differentiation. Genes Dev. 2003 Aug 15;17(16):1979-91. PubMed PMID: 12923053. Pubmed Central PMCID: 196253.

35.   Tajima K, Takaishi H, Takito J, Tohmonda T, Yoda M, Ota N, et al. Inhibition of STAT1 accelerates bone fracture healing. J Orthop Res. 2010 Jul;28(7):937-41. PubMed PMID: 20063384.

36.   Zhou Y, Tan L, Que Q, Li H, Cai L, Cao L, et al. Study of association between HLA-DR4 and DR53 and autoantibody detection in rheumatoid arthritis. Journal of immunoassay & immunochemistry. 2013;34(2):126-33. PubMed PMID: 23537298.

37.   van der Heijde D, Tanaka Y, Fleischmann R, Keystone E, Kremer J, Zerbini C, et al. Tofacitinib (CP-690,550) in patients with rheumatoid arthritis receiving methotrexate: twelve-month data from a twenty-four-month phase III randomized radiographic study. Arthritis and rheumatism. 2013 Mar;65(3):559-70. PubMed PMID: 23348607.
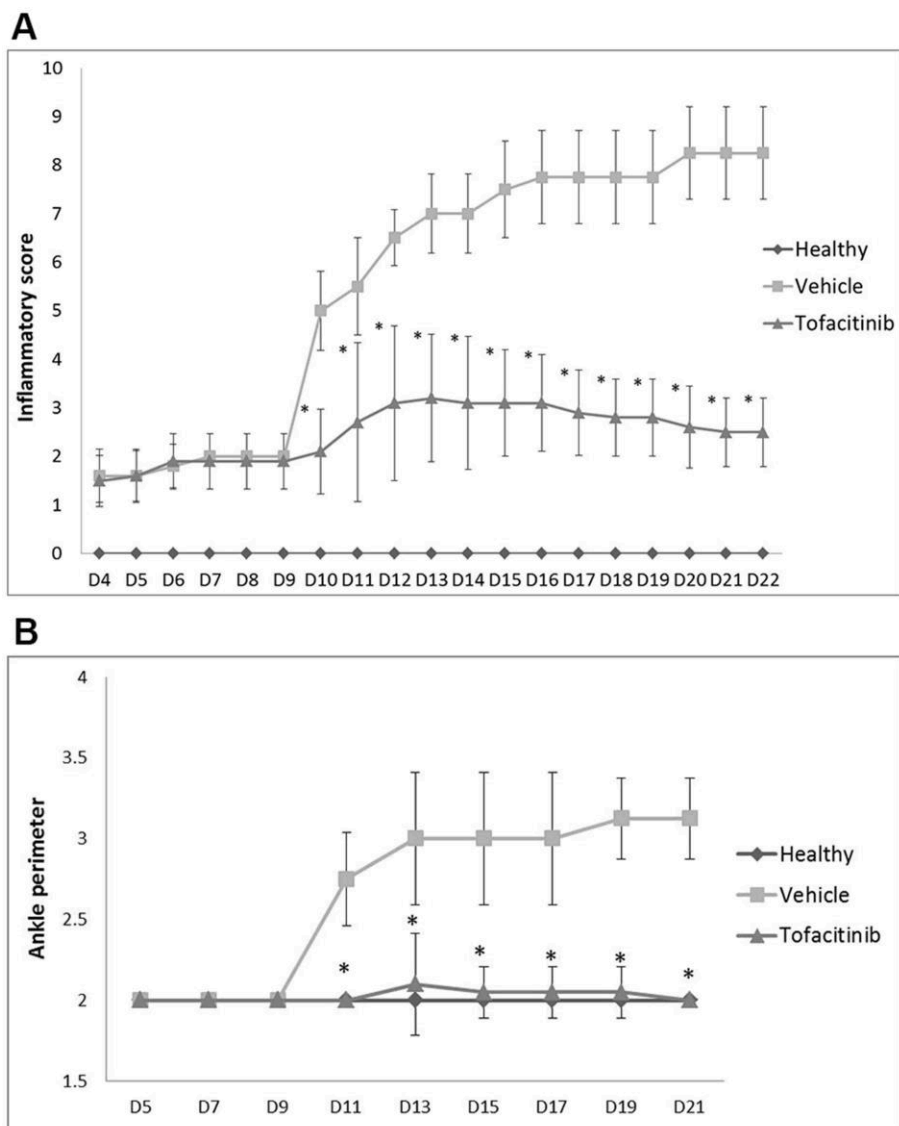
Image 1 – Inflammatory score and ankle perimeter. (A) Inflammatory score - Tofacitinib group was compared with the vehicle group (arthritic). Results showed statistical differences throughout time since day 10 p= 0.0071 up to day 22 p= 0.0058. (B) Ankle perimeter. Tofacitinib group was compared with the vehicle group (arthritic). Results showed statistical differences throughout time since day 11 p= 0.0057 up to day 22 p= 0.0056. Statistical differences were determined with non-parametric Mann Whitney test using GraphPad Prism (GraphPad, California, USA). Differences were considered statistically significant for p values ≤ 0.05. Healthy N=20, Arthritic N=20, Tofacitinib N=10.
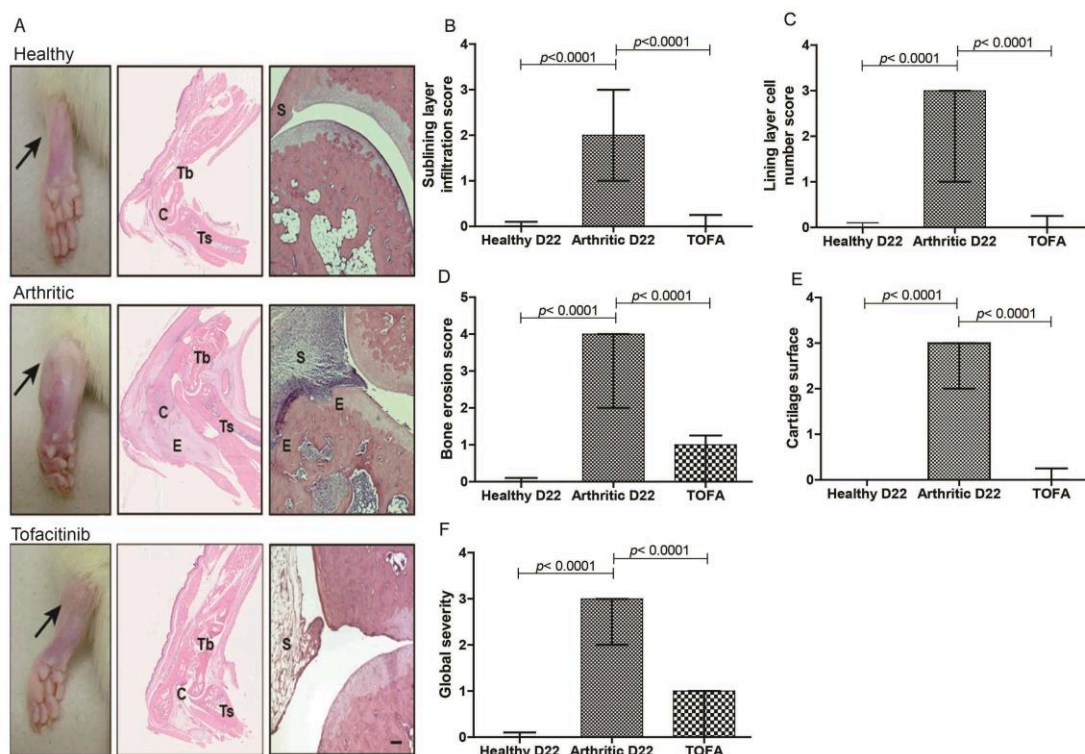
Image 2 – (A) Histological images of joints after tofacitinib treatment. These patterns are merely illustrative of the type of histological features observed. Black arrow indicates the absence/presence of ankle swelling in rat hind paws. C–calcaneus, E–edema or erosion, S–synovia, Tb–tibia, Ts–tarso. Magnification of 50X. Bar: 100 µm. Tofacitinib suppressed inflammation and tissue damage locally in the joints of AIA rats. A semi-quantitative evaluation of histological sections was performed. Notice that tofacitinib inhibited cellular infiltration (B), completely reversed the number of lining layer cells to the normal values (C) and prevented bone erosion occurrence (D), allowing for a normal cartilage (E) and joint structure, comparable to healthy rats (F). Data are expressed as median with interquartile range. Differences were considered statistically significant for p-values<0.05, according to Mann Whitney test. Healthy N=20, Arthritic N=20, Tofacitinib N=10.
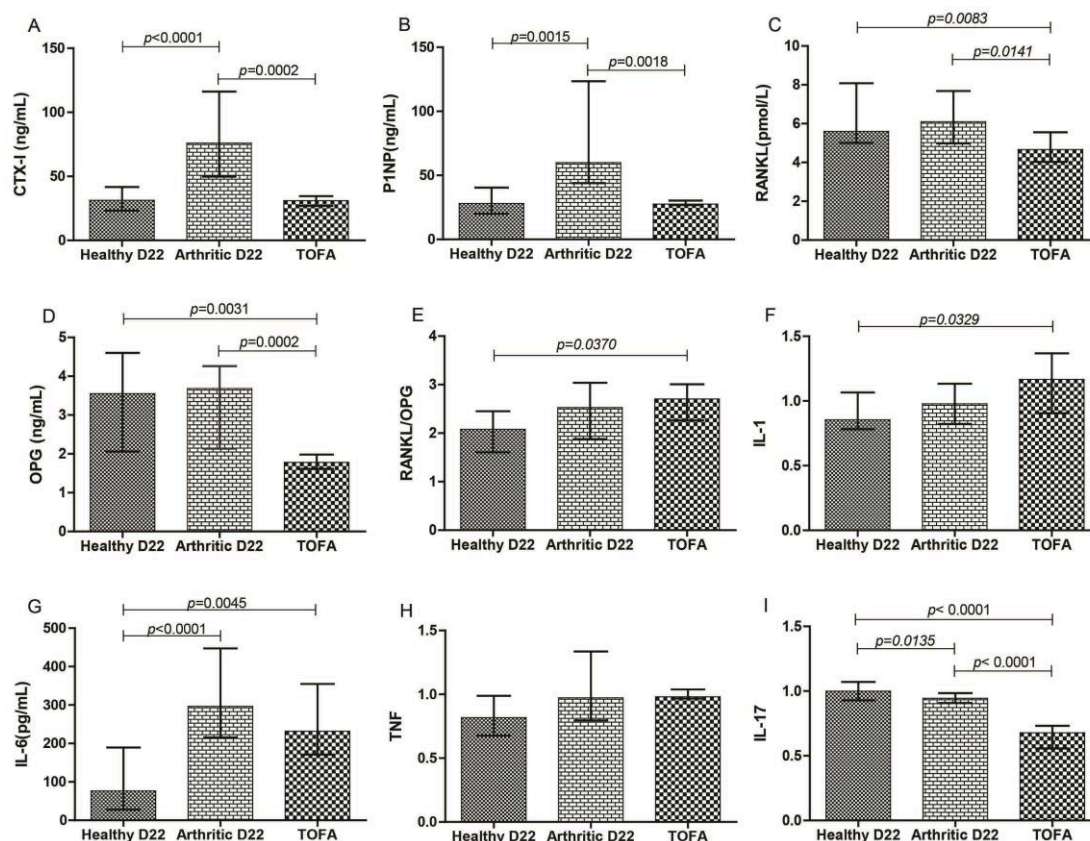
Image 3 - Bone turnover markers and systemic cytokines quantifications. Serum samples collected at day 22 (sacrifice) were analyzed by ELISA technique. Bone resorption marker, CTX-I (A) and bone formation marker, P1NP (B) were increased in arthritic rats (p<0.0001 and p = 0.0015, respectively). Tofacitinib group showed decreased values for CTX-I (p= 0.0002) and P1NP (p= 0.0018). RANKL (C) and OPG (D) were diminished in tofacitinib treated rats when compared to arthritic untreated group (p= 0.0141 and p= 0.0002, respectively). RANKL/OPG ratio (E) showed higher values when compared to healthy group (p= 0.0370).

Tofacitinib, in this animal model, did not affect circulating levels of IL-1 β (F) and TNF (H). Results have also demonstrated a significant decrease in the serum quantification of IL-17 (I) (p<0.0001) and a tendency towards a decrease of IL-6 (G). IL-1, TNF and IL-17 were normalized. Differences were considered statistically significant for p-values<0.05, according to the Mann Whitney tests. Healthy N=20, Arthritic N=20, Tofacitinib N=10.
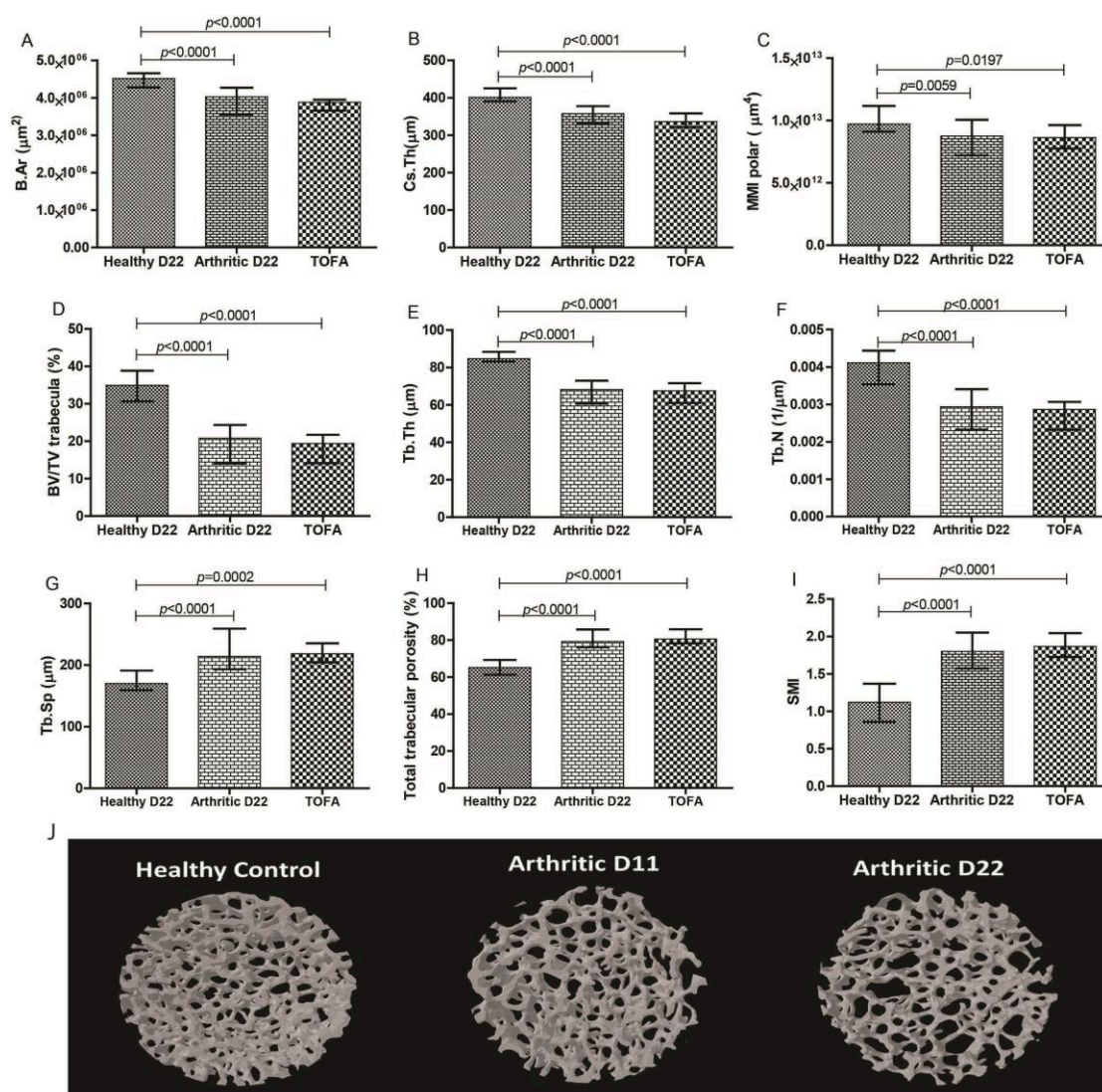
14

Image 4 – Micro-computed tomography (micro-CT) analysis of tibiae rat sample.

The arthritic and tofacitinib groups showed decreased values for cortical crossectional bone area (A), thickness (B) and polar moment of inertia (C) when compared to healthy controls. Trabecular bone also showed lower values of ratio bone volume/tissue volume (D), trabecular thickness (E) and number (F) in comparison with healthy controls. Arthritic and tofacitinib rats demonstrated higher values of trabecular separation (G) and porosity (H) when compared to healthy controls. Structural model index showed decreased values in arthritic and tofacitinib rats in comparison to healthy rats. MicroCT images from healthy, arthritic untreated and tofacitinib tibiae rats (J). Images acquired with SkyScan 1272, Bruker microCT, Kontich, Belgium. Differences were considered statistically significant for p-values<0.05, according to the Mann–Whitney tests. Healthy N=20, Arthritic N=20, Tofacitinib N=10.
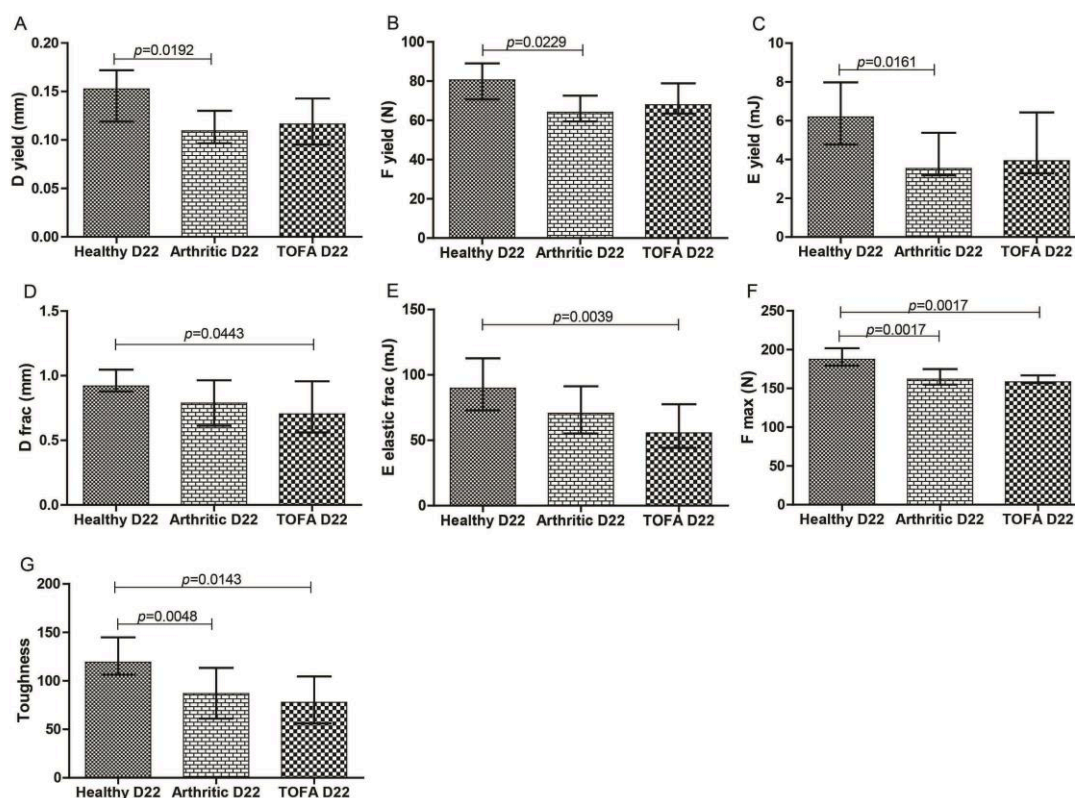
Image 5 – Bone mechanical properties assessed by three-point bending tests in rat femur at 22 days post disease induction.

Results showed that arthritic rats have decreased properties at yield point, related to displacement (A), strength (B) and pre yield energy (elastic energy) (C). Tofacitinib treated rats had a significant decrease in displacement (D) and elastic properties (E) at fracture point. Arthritic and tofacitinib treated bones required a lower maximum load (F) to fracture and a decreased toughness (G) was observed. Differences were considered statistically significant for p-values<0.05, according to the Mann–Whitney tests. Healthy N=20, Arthritic N=20, Tofacitinib N=10.
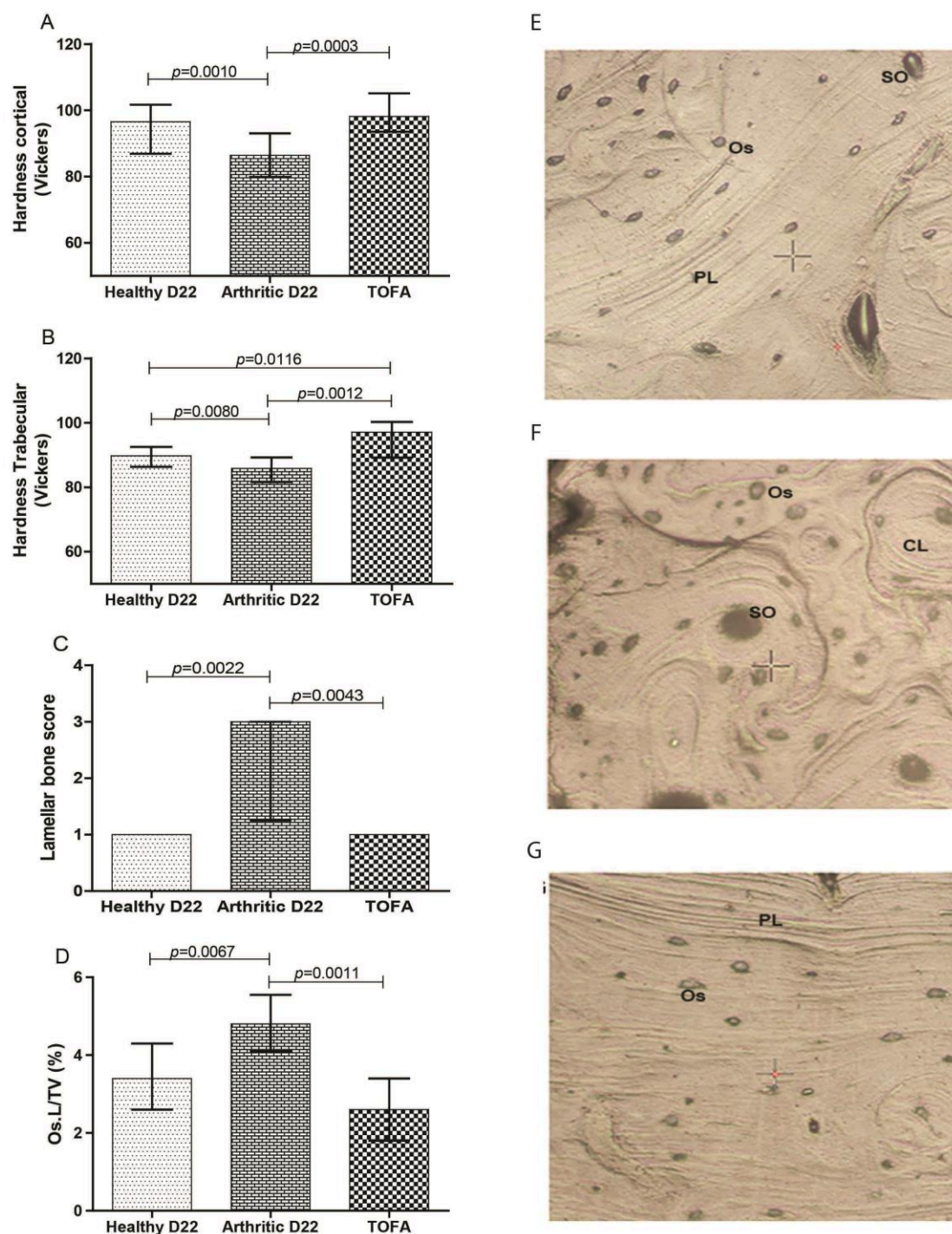
Image 6 – Bone mechanical properties assessed by nanoindentation in rat femur at 22 days post disease induction and respective topographic images from the indentation tissue area. Nano-mechanical tests revealed a decreased cortical (A) and trabecular (B) hardness in arthritic group at day 22 when compared to healthy rats. Of notice, rats treated with tofacitinib showed increased hardness in cortical (A) and trabecular (B) bone in comparison with untreated arthritic rats. Results demonstrated that the number of concentric lamellae (C) and ratio of area occupied by osteocyte lacunae in the total tissue (D) were higher when compared to healthy controls and tofacitinib treated groups at day 22.

Images are merely illustrative of the type of histological features observed. Concentric lamellas were identified in secondary osteons (SO), characteristic from arthritic animals (F). On the

contrary, parallel-lamellae (PL) were identified in healthy controls (E) and tofacitinib treated groups (G). Os – Osteocytes, SO – Secondary osteons, PL – Parallel-lamellae, CL – Concentric lamellas. Magnification 20X. Differences were considered statistically significant for p-values<0.05, according to the Mann–Whitney tests. Healthy N=20, Arthritic N=20, Tofacitinib N=10.

Supplementary data
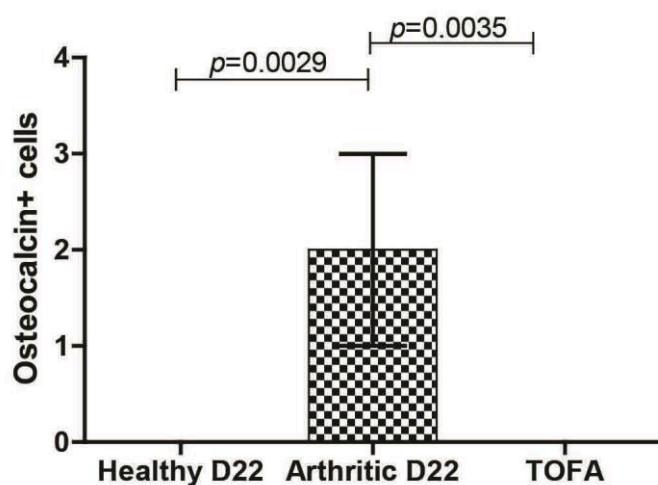
Supplementary figure 1 - Tofacitinib reduces the number of osteoblasts.

Immunohistochemical analysis was performed using a semi-quantitative score. Notice that tofacitinib treated rats showed a significant reduction in the number osteocalcin positive cells in comparison with arthritic rats at day 22. Healthy N = 10, Arthritic N = 10, Tofacitinib treated group N = 10. Data are expressed as median with interquartile range. Differences were considered statistically significant for p-values<0.05, according to the Mann–Whitney tests.
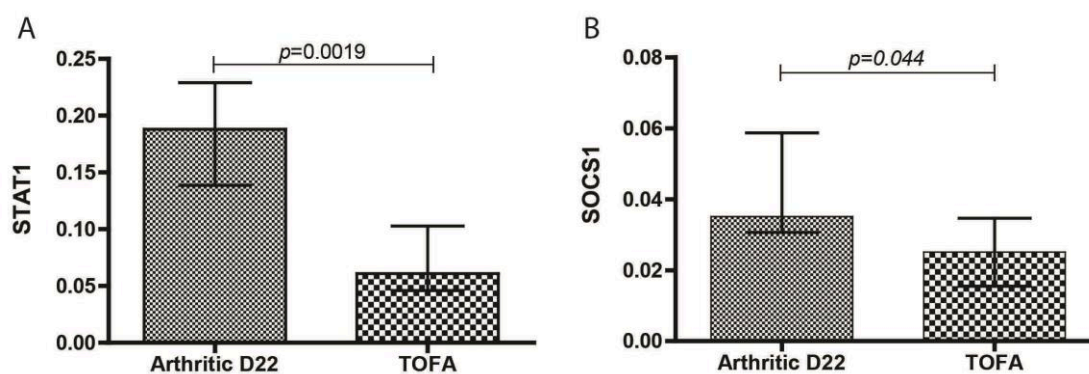
Supplementary figure 2 – Tofacitinib down-regulates the expresision of JAK-STAT pathway.

STAT1 (A) and SOCS1 (B) quantified by quantitative qPCR. Notice that tofacitinib down-regulates the JAK-STAT pathway with a significant decreased expression of STAT1 and SOCS1 in tofacitinib treated rats when compared to arthritic rats at day 22. Arthritic N = 14, Tofacitinib treated group N = 10. Data are expressed as median with interquartile range. Differences were considered statistically significant for p-values<0.05, according to the Mann–Whitney tests.

RHEUMATOLOGY

Corrigendum

Effects of tofacitinib in early arthritis-induced bone loss in an adjuvant-induced arthritis rat model

Bruno Vidal[1], Rita Cascão[1], Mikko A.J. Finnilä[2,3], Inês P. Lopes[1], Vânia G. da Glória[1], Simo Saarakkala[2,4], Peter Zioupos[5], Helena Canhão[6] and João Eurico Fonseca[1,7]

Figure 4J was missing the photo of tofacitinib effect on bone. The Figure has been corrected and the corrected image also appears below.

Fig. 4 Micro-CT analysis of samples of rat tibia
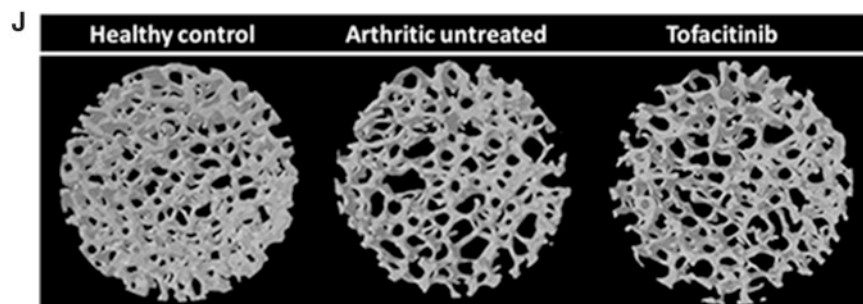
The arthritic and tofacitinib groups showed decreased values for cortical cross-sectional bone area (**A**), thickness (**B**) and polar moment of inertia (**C**) when compared with healthy controls. Trabecular bone also showed lower values of ratio bone volume/tissue volume (**D**), trabecular thickness (**E**) and number (**F**) in comparison with healthy controls. Arthritic and tofacitinib rats demonstrated higher values of trabecular separation (**G**) and porosity (**H**) when compared with healthy controls. The structural model index showed decreased values in arthritic and tofacitinib rats compared with healthy rats. Micro-CT images from tibias of healthy, arthritic untreated and tofacitinib groups (**J**). Images were acquired with SkyScan 1272 (Bruker microCT, Kontich, Belgium). Differences were considered statistically significant for $P < 0.05$, according to the Mann–Whitney U-test. Healthy: n = 20; arthritic: n = 20; tofacitinib: n = 10.

CORRIGENDUM

[1]Instituto de Medicina Molecular, Faculdade de Medicina, Universidade de Lisboa, Lisbon, Portugal, [2]Research Unit of Medical Imaging, Physics and Technology, Faculty of Medicine, University of Oulu, Oulu, [3]Department of Applied Physics, University of Eastern Finland, Kuopio, [4]Medical Research Center, University of Oulu, Oulu, Finland, [5]Biomechanics Laboratories, Cranfield Forensic Institute, Cranfield University, Defence Academy of the UK, Shrivenham, UK, [6]CEDOC, EpiDoC Unit, NOVA Medical School and National School of Public Health, Universidade Nova de Lisboa, Lisboa, Portugal and [7]Rheumatology Department, Centro Hospitalar de Lisboa Norte, EPE, Hospital de Santa Maria, Lisbon Academic Medical Centre, Lisbon, Portugal

Correspondence to: Bruno Vidal, Instituto de Medicina Molecular, Faculdade de Medicina da Universidade de Lisboa, Av. Professor Egas Moniz, 1649-028 Lisboa, Portugal.
E-mail: vidal.bmc@gmail.com